Wetland monitoring using classification trees and SPOT-5 seasonal time series

Aurélie Davranche, Gaëtan Lefebvre, Brigitte Poulin

Wetland monitoring using classification trees and SPOT-5 seasonal time series.

Aurélie Davranche[1]*, Gaëtan Lefebvre[2], Brigitte Poulin[2]

[1] Institut für Geographie, Friedrich-Alexander Universität Erlangen-Nürnberg, Haberstr. 2, 91054 Erlangen, Germany

[2]Tour du Valat Research Center, Le Sambuc, 13200 Arles, France

*Corresponding author. Tel.: ++49 (0)9131/85-2 52 41, FAX: ++49 (0)9131/85-2 52 28.

E-mail address: adavranche@geographie.uni-erlangen.de

Abstract

Multi-season reflectance data from radiometrically and geometrically corrected multispectral SPOT-5 images of 10-m resolution were combined with thorough field campaigns and land cover digitizing using a binary classification tree algorithm to estimate the area of marshes covered with common reeds *(Phragmites australis)* and submerged macrophytes *(Potamogeton pectinatus, P. pusillus, Myriophyllum spicatum, Ruppia maritima, Chara sp.)* over an area of 145 000 ha. Accuracy of these models was estimated by cross-validation and by calculating the percentage of correctly classified pixels on the resulting maps. Robustness of this approach was assessed by applying these models to an independent set of images using independent field data for validation. Biophysical parameters of both habitat types were used to interpret the misclassifications. The resulting trees provided a cross-validation accuracy of 98.7% for common reed and 97.4% for submerged macrophytes. Variables discriminating reed marshes from other land covers were the difference in the near-infrared band between March and June, the Optimized Soil Adjusted Vegetation Index of December, and the Normalized Difference Water Index (NDWI) of September. Submerged macrophyte beds were discriminated with the shortwave-infrared band of December, the NDWI of September, the red band of September and the Simple Ratio index of March. Mapping validations provided accuracies of 98.6% (2005) and 98.1% (2006) for common reed, and 86.7% (2005) and 85.9% (2006) for submerged macrophytes. The combination of multispectral and multisesasonal satellite data thus discriminated these wetland vegetation types efficiently. Misclassifications were partly explained by digitizing inaccuracies, and were not related to biophysical parameters for reedbeds. The classification accuracy of submerged macrophytes was influenced by the proportion of plants showing on the water surface, percent cover of submerged species, water turbidity, and salinity. Classification trees applied to time series of SPOT-5 images appear as a powerful and reliable

tool for monitoring wetland vegetation experiencing different hydrological regimes even with a small training sample (N = 25) when initially combined with thorough field measurements.

Keywords: Camargue, classification tree, multispectral indices, multitemporal indices, Phragmites australis, remote sensing, SPOT-5, submerged macrophytes, wetland monitoring.

1. Introduction

Efficient, accurate and robust tools for monitoring wetlands over large areas are urgently needed following their destruction and degradation, in spite of the many services and functions they provide to human kind (Özesmi & Bauer, 2002). Accurate wetland mapping is an important tool for understanding wetland functions and monitoring their response to natural and anthropogenic actions (Baker et al, 2006).

Satellite remote sensing increasingly presents many advantages for inventorying and monitoring all types of wetlands (Özesmi & Bauer, 2002). Unsupervised classification or clustering is the most commonly used digital classification to map wetlands with multispectral data, while the maximum likelihood algorithm is the most frequently used method for supervised classification. Low wetland accuracies (30 – 60%) often result from these classification methods (Özesmi, 2000; but see Macalister and Mahaxy, 2009). Multi-temporal, multi-spectral, ancillary data or a rule-based approach are expected to provide better results than traditional image processing techniques (Özesmi & Bauer, 2002)

Many wetland species have overlapping spectral reflectances at peak biomass (Schmidt & Skidmore, 2003) and aggregation of similar wetland classes are sometimes necessary to achieve better accuracies (Wright & Gallant, 2007). Hence, a multiseasonal imagery can be most useful

for distinguishing plant species within a single growing season (Ghioca-Robrecht et al., 2008), further integrating seasonal variability in water regimes and vegetation (Özesmi & Bauer, 2002). For instance, Ramsey & Laine (1997) have demonstrated that the combination of images from two seasons facilitates the segregation between emergent and floating vegetation (winter and spring), and between flooded emergent vegetation and open water (fall and winter).

Multispectral data have also been used as an alternative approach for wetland plant discrimination with satellite remote sensing (Özesmi & Bauer, 2002). Johnston & Barson (1993) observed that using simple density slicing of bands that are related to physical parameters such as vegetation indices, mid infrared and visible blue may be as effective as more complicated statistical classification. Multispectral indices (addition, subtraction, multiplication or division of pixel brightness between two bands) are also expected to improve models for wetland discrimination (Bradley & Fleishman, 2008) because they are sensitive to vegetation surface roughness, its moisture conditions and stage of development.

Non-parametric classifiers such as rule-based methods are an increasingly used alternative to traditional remote sensing techniques to enhance the accuracy of wetland classification (Sader et al., 1995; Özesmi, 2000; Baker et al., 2006). Because classification trees (CTs) easily accommodate data from all measurements scales, they are useful for distinguishing spectral similarities among wetlands with ancillary environmental data (Wright & Gallant, 2007). Resampling statistical methods such as bagging (bootstrap aggregation) and boosting can improve CT accuracy, but they also make the interpretation of the results more complex (Lawrence et al., 2004).

Flooded areas pose unusual challenges for field campaigns, and class imbalance in remote sensing of wetlands is a well-known problem (Wright & Gallant, 2007). Spatial studies of these ecosystems require flexible and robust analytical methods to deal with non-linear relationships,

high-order interactions, and missing data. Despite such difficulties, methods used for mapping the distribution of wetlands should be simple to understand and easy to interpret in order to contribute to management advising. Seasonal time series of satellite multispectral data may provide, through the use of CTs, reliable, replicable and understandable tools for a wetland mapping and follow-up. The aim of this study is to evaluate the potential of CTs and multiseasonal SPOT-5 images to model the presence of dominant emergent and submerged macrophytes of Camargue marshes. The ultimate goal is to provide a re-applicable remote-sensing tool for their long-term monitoring to assist management decisions that will insure a good balance between economic interests and nature conservation.

2. Methods

2.1. Study area

The study area is the Camargue or Rhône delta covering 145 000 ha near the Mediterranean Sea in southern France (Fig. 1). The Camargue consists mainly of agricultural land (mostly rice) mixed with natural or semi-natural brackish marshes either covered with submerged marcrophytes (*Potamogeton, Myriophyllum, Ruppia, Chara*) or tall helophytes (mostly common reed *Phragmites australis* but also club-rush *Bolboschoenus maritimus, Schoenoplectus littoralis, S. lacustris* and cattail *Typha angustifolia, T. latifolia)*. The climate is Mediterranean with mild and windy winters and hot and dry summers. Mean annual rainfall over the last 30 years is 579 ± 158 (SD) mm, being concentrated in spring and autumn, with large intra- and inter-annual variations (Chauvelon, 2009). The Camargue has lost 40 000 ha of natural areas, including 33 000 ha of wetlands over the last 60 years, following the extension of agriculture, salt exploitation and industry (Tamisier & Grillas, 1994). A large part of the

remaining marshes, located on private estates, has been fragmented and intensively managed through freshwater inputs for socio-economic activities such as waterfowl hunting, reed harvesting, and cattle grazing. The increased hydroperiod of these marshes results in a loss of their Mediterranean flora and fauna, which are well adapted to summer droughts (Tamisier & Grillas, 1994). Vegetation development and density in Camargue marshes is influenced by physical factors such as salinity, water depth, and water level fluctuations, which have an effect on reflectance spectra (Silvestri et al., 2002).

2.2. Habitat description

In the Camargue, common reed *(Phragmites australis)* can form monospecific stands over large areas in shallow marshes or develop linearly along canals. Aerial stems emerge during spring and reach their maximum growth at the end of June. The inflorescences or panicles start developing in July and turn purplish-brown with a fluffy aspect at maturation in autumn. Seeds are wind-dispersed in early winter with the panicles becoming thinner and switching to a beige colour. Leaves remain green until October and turn yellow before drying and falling down in winter. The stems then dry but stand for a few years before breaking down. In order to provide sustainable conditions for reed harvesting in winter, reedbeds are flooded from March to June, dried in summer, flooded in autumn and drained in winter for mechanical harvest (December – March). Flooding can be extended through spring or summer if waterfowl hunting occurs. The total area of reedbeds in the Camargue is estimated at about 8000 ha, of which 2000 ha is harvested every year (Mathevet & Sandoz, 1999).

Beds of submerged macrophytes develop in unmanaged marshes that dry in summer as well as in marshes managed for waterfowl hunting, which are either permanently flooded with freshwater inputs or drained shortly in spring (Tamisier & Grillas, 1994). These open marshes,

which vary in size from 0.02 ha to 250 ha, can develop dense mono- or multispecific stands of pondweeds (*Potamogeton pectinatus*, *Potamogeton pusillus*), Eurasian water milfoils (*Myriophyllum spicatum*) or widgeon grasses (*Ruppia maritima*). Some *Chara* spp. characteristic of unmanaged marshes can develop in spring but are generally quickly replaced by the species mentioned above that are more competitive in quasi-permanently flooded marshes. Thus, depending upon the water management and the species, submerged macrophytes develop from mid-February to late March, reaching their maximum growth in May through July. A progressive senescence starts from early winter but some plants can remain until the next spring. Water inputs generating new emergence can also be observed in autumn. Water turbidity is generally low because submerged plants limit sediment movement. A continuous surficial water flow is sometimes favoured by managers to increase marsh attractiveness to ducks. The total area of submerged macrophytes in the Camargue has not been estimated.

2.3. Field sampling

2.3.1. Reed and submerged macrophyte beds

Physical access to many wetlands was hindered by water too shallow for boat access and by roads too bad for vehicle access. The difficulties associated with the sampling of remote flooded marshes were further hampered by land privacy. Selection of study plots was a compromise between admittance, accessibility, and getting a representative sample of the Camargue marshes based on aerial photographs and videos collected during flights by plane or ultra-light motorized engines (ULM). The number of plots surveyed was further limited by the relatively short sampling period of optimal plant growth. The training sample, collected in 2005, consisted of 46 plots of common reed and 25 plots of submerged macrophytes spread throughout the Camargue (Fig. 1). The independent validation sample of 2006 consisted of 21 sites of

145 common reed, and 83 sites of aquatic beds. All study plots were located in seasonal or permanent
146 shallow marshes either covered with reed-dominated helophytes or with submerged macrophytes
147 during some time of the year.

148 For each habitat type, water and vegetation measures were taken within 20 X 20 m
149 squares (i.e., four pixels of a SPOT-5 scene) of homogeneous vegetation placed within a larger
150 homogeneous zone and located at least 70 m from the border to reduce edge effects in spectral
151 response.. Plot size was defined in order to contain at least one pure pixel (10 X 10 m) of a
152 SPOT-5 scene. Each sampling plot was placed in a different hydrological unit to increase
153 structural diversity and avoid autocorrelation. They were geolocated with a GPS (Holux GR-
154 230XX) situated in the centre of the plot at three meters above ground to avoid interferences
155 caused by high reed stems, using the average position obtained during the whole process of field
156 data gathering (1-2 hours). Water level, plant cover and composition were estimated along two
157 diagonals crossing the entire plot between May and July, depending upon the development of the
158 vegetation. Common reed density was measured by counting the green and dry stems inside four
159 quadrats of 50 X 50 cm per plot in June or July located at seven meters from the center of the plot
160 in each cardinal direction. Homogeneity throughout the plot was visually estimated and coded
161 from 1 to 4. Vegetation cover was evaluated with four digital pictures taken vertically from the
162 ground level upwards in the centre of the 50-cm quadrats and processed with CANEYE (Baret &
163 Weiss, 2004), a software that derive canopy characteristics such as LAI, fAPAR and the cover
164 fraction with several photographs. The estimation of the canopy characteristics are based on the
165 transmittance of light through the canopy considering the vegetation elements as opaque (Baret &
166 Weiss, 2004).

167 Water levels were measured at a permanent rule during vegetation sampling, as well as
168 monthly or twice monthly at each hydrological unit sampled.

2.3.2. Other land covers

Tamarisk (*Tamarix gallica*), riparian forest, rush, grassland, sand (dune or beach), salt pan, saline marsh (more or less covered by perennial halophytes such as *Arthrocnemum spp*), other forests (including pine forest), agricultural and urban areas were extracted from a vector layer created by the Réserve Nationale de Camargue from aerial photographs in 2001 provided by the Parc Naturel Régional de Camargue. Additional categories were digitized based on aerial photographs and ground or aerial (airplane and ultra-light aircrafts) surveys: sea, rice, sawgrass (*Cladium mariscus*), club rush (*Bolboschoenus maritimus, Schoenoplectus littoralis, S. lacustris*), cattails *(Typha spp.)*, and groundsel bush *(Baccharis halimifolia)*. In 2006, an updated land cover was available, providing details for agricultural crops. Homogenous stands of groundsel bush and cattails were unfortunately too few to be included in the validation sample. We therefore obtained a total of 640 polygons for the training sample and 587 polygons for the validation sample.

2.4. Image processing

The Camargue can be covered with a single SPOT-5 scene (60 X 60 km). Two seasonal time series of SPOT-5 images (SPOT/Programme ISIS. Copyright CNES) and field data sets were acquired at one year intervals for model building (2004-2005) and validation (2005-2006). Thanks to the Spot satellite programming service, scenes were acquired in late December, March, May, June, July and September (October in 2006) of both years. These dates had been selected based on vegetation phenology and seasonal water management of the targeted habitats. The programming service provided several possible images within a two-week period when meteorological conditions were not optimal. SPOT-5 has 10-m spatial resolution and four bands: B1 (green: 0.50 to 0.59 µ m), B2 (red: 0.61 to 0.68 µ m), B3 (near-infrared NIR: 0.79 to 0.89 µ m) and B4 (shortwave-infrared SWIR: 1.58 to 1.75 µ m). Spot scenes came with radiometric

193 correction of distortions due to differences in sensitivity of the elementary detectors of the
194 viewing instrument that is the preprocessing level called 1A (Spot image, 2008).
195 Scenes were radiometrically normalized using the 6S atmospheric code (Davranche et al.,
196 2009) developed by Vermote et al. (1997), and projected to Lambert conformal conic projection
197 datum NTF (Nouvelle Triangulation Française) using a second-order transformation and nearest-
198 neighbour re-sampling. The scenes were georeferenced to a topographic map at 1:25, 000 scale.
199 We extracted the mean reflectance value for each plot of reed and aquatic beds and each polygon
200 of other land covers from each band of each scene using the 'Spatial Analyst' of ArcGis version
201 9.2 (Environmental Systems Research Institute, Meudon, France). Using these data, we further
202 calculated for each plot and polygon the most common multispectral indices (Table 1), and
203 multitemporal indices corresponding to subtractions between each pair combination of dates. In
204 the data file, these variables were labelled as follow: OSAVI_12 for the Optimized Soil Adjusted
205 Vegetation Index of December and B3_0603 for the difference between March and June in the
206 reflectance value of band B3.
207
208 *2.5. Statistical modelling and mapping*
209 *2.5.1 Classification trees*
210 CT analyses based on dichotomous partitioning (Breiman et al., 1984) were performed with
211 the Rpart (Recursive PARTitioning, Therneau & Atkinson, 1997) package in the R software
212 using a class coded "1" for the presence of reed or submerged macrophyte beds and a class coded
213 "0" for absence (= other land cover types detailed in 2.4.2). This method is less sensitive to data
214 fragmentation than multivariate classification trees (Brostaux, 2005) and uses the cost-complexity
215 parameter (*cp*) for pruning.
216 For the pruning phase, we tested two cross-validation procedures CV-0SE and CV-1SE,

217 described by Esposito et al. (1999). Cross-validation is well suited to small samples, but can also
218 improve results for large data sets (Breiman et al., 1984). For both methods, we used 10 cross-
219 validation subsets, which is the recommended default value by Breiman et al. (1984). The
220 optimally pruned tree was defined with the *cp* providing the smallest overall classification error
221 rate among 10 iterative runs of the algorithm. To improve classification accuracies with our
222 unbalanced samples, the optimal prior parameter that gives the highest classification accuracy
223 was selected using the iterative method proposed by Breiman et al. (1984).
224
225 *2.5.2. Map validation*
226 The equations issued from the resulting trees were applied to SPOT-5 scenes of 2005 for
227 estimating model accuracy and to 2006 scenes for estimating model robustness. For this
228 procedure we used the raster calculator (Spatial Analyst) of ArcGIS to create binary maps, with 1
229 encoded for the presence of reed or aquatic beds and 0 for the presence of other land covers.
230 Using the zonal statistics tool (Spatial Analyst) of ArcGIS, we extracted the values 1 and 0 for
231 each class of the validation sampling. As described by Wright & Gallant (2007), overall
232 accuracies and omission error rates were calculated using the sample error matrix, whereas the
233 commission and overall error rates were estimated from the population error matrix given known
234 numbers of reedbeds, aquatic beds and other land covers in the study area for each map. We
235 further calculated the omission error rates for the different categories of the other land cover in
236 the validation sample. The resulting distribution maps were confronted with expert knowledge
237 and additional field visits for interpretation of potentially misclassified areas.
238
239
240

241 *2.5.3 Relevance of the models and interpretation of misclassifications*

242 To test the relevance of the variables selected in both models, their mean value and 95%
243 confidence intervals were calculated for each class of the training and the validation samples. The
244 binary response (0/1) for miss-classified and well-classified plots in both years was confronted to
245 structural parameters of reed or submerged macrophytes considered individually, using the
246 likelihood ratio test (Sokal & Rohlf, 1995) for model significance. This test is considered as more
247 reliable than the Wald test with small samples (Harrell, 2001). The following parameters were
248 examined for common reed: height of green stems, density of green and dry stems, dry-to-green
249 stem ratio, diameter of green and dry stems, plot homogeneity, and percent cover of vegetation.
250 For submerged macrophytes, the parameters used were: percent cover of the vegetation,
251 dominant plant species, water level, water turbidity, and proportion of submerged plants showing
252 on the water surface. For both habitats, a year variable was included as a potential parameter for
253 misclassification.

254

255 **3. Results**

256

257 *3.1. Models*

258 The resulting classification tree for common reed (Fig. 2) provided a cross-validation
259 accuracy of 98.7% with the equation: B3_0603 $\geq$ 0.04897 and OSAVI_12 < 0.2467 and
260 MNDWI_09 < -0.3834. The resulting classification tree for submerged vegetation (Fig. 3)
261 provided a cross-validation accuracy of 97.4% with the equation: **(**B4_12 < 0.05355 and
262 NDWIF_09 < 0.2466 and B2_09 < 0.07147) or (B4_12 $\geq$ 0.05355 and SR_03 $\geq$ 0.9827). The
263 CV-1SE pruning method offered the best results. The best prior parameter was 0.40 for the class
264 “0” and 0.60 for the class “1” in both models.

265 *3.3. Mapping validation*

266 The map of common reed resulted in an overall accuracy of 98.6% in 2005 and 98.1% in
267 2006 (Table 2, Figs. 4-5). Common reed sites were incorrectly classified at 16.7% in 2005 and
268 11.5% in 2006. Misclassifications involved mostly tamarisks on both years, as well as club rush
269 and sunflower in 2006 (Table 3). Considering the omission error rates of both classes, the total
270 area covered by common reed in the Camargue is estimated at 8842 ha in 2005 and 9128 ha in
271 2006.

272 The overall accuracy of the submerged-macrophyte map was 86.7% in 2005 and 85.9% in
273 2006 (Table 2 & Figs. 4-5). Submerged macrophyte sites were incorrectly classified at 10.1% in
274 2005 and 16.2% in 2006. Misclassifications involved mostly club-rush and saline marshes on
275 both years (Table 3), leading to commission error rates of 25 to 41% higher than those of
276 reedbeds (Table 2). Considering the omission error rates of both classes, the total area covered by
277 submerged macrophytes in the Camargue is estimated at 29 244 ha in 2005 and 33 797 ha in
278 2006.

279

280 *3.4. Robustness of the models and misclassification interpretation*

281 The variables selected in the models exhibited a similar range of variation in 2005 and
282 2006, suggesting that our approach might be robust for inter-annual applications. The 95%
283 confidence interval of most variables for reed and submerged macrophyte beds was far from the
284 splitting values used for classification (Figs. 6-9). The only exceptions were the lowest values of
285 the NDWIF in October and the highest values of the SR index in March for classifying
286 submerged macrophytes on both years.

287 None of the measured structural parameters of reeds could explain their misclassification,
288 which was nevertheless associated to the year (Table 4), with a better classification in 2005

289 (training sample). Classification of submerged macrophytes was influenced by proportion of
290 plants showing on the water surface, percent cover of submerged species, water turbidity,
291 salinity, and to a lesser extent the year (Table 4). The best conditions for submerged macrophyte
292 classification were high percentage of plant cover with low turbidity and salinity in 2005.
293 Following the confusion with seagrass *(Zostera noltii)* in the Vaccarès lagoon in 2006, we further
294 calculated the NDWIF values of September and October for presumed seagrass in the Vaccarès
295 and observed that they were well below the minimal splitting rule (≥ 0.2466) of the CT in
296 October (0.09 – 0.12) but not September (0.32 – 0.38).
297
298 **4. Discussion**
299 Although no additional environmental ancillary data or new methods to address the
300 shortcomings of CT were used in this study, the combination of multispectral and multiseasonal
301 remotely-sensed data provided a good discrimination of wetland vegetation. The fact that CTs
302 can process a large amount of data without requiring a pre-selection of variables facilitates their
303 application and allowed us to create simple models. The predictive variables involved in the
304 models were linked to the hydrology and plant phenology known to influence the spectral
305 responses of costal wetland vegetation (Caillaud et al., 1998). For reedbed discrimination,
306 difference of the B3 between March and June was linked to their chlorophyll production, which
307 is particularly high in summer and low in winter (Caillaud et al., 1998; Valta-Hulkkonen et al.,
308 2003). The OSAVI of December probably reflected the high homogeneity of dry reed stands in
309 winter that presents a uniform reddish-brown colour. This index is recognised as a good tool for
310 highlighting homogeneous grass or agricultural crop canopies at mid latitudes (Rondeaux et al.,
311 1996), and presents similar values for ploughed crops, rice cultivation, sand and sunflower that
312 have a comparable uniform colour in December in the Camargue. The MNDWI provides

313 negative values for soil and vegetation, and positive values for water (Hanqiu, 2006). Its selection
314 in September could be related to the specific response of panicles and/or the water inputs that
315 decrease the near and shortwave infrared values. Because the values of MNDWI in September for
316 reed and groundsel bush are close, a specific response of the panicles is likely to explain the
317 selection of this variable in the model. The groundsel bush grows on dikes where water levels
318 have no influence. Its terminal and conspicuous inflorescences are white to pale yellow in
319 autumn, and are expected to provide a similar spectral response to that of reed inflorescences in
320 late September. Moreover, some MNDWI values of cattail plots were also in the range of the
321 reed values in September. When ripen in fall, the cattail inflorescences consist of golden to brown
322 fluffy hairs attached to the tip of the shoot.

323 Confusion between tamarisk and reed in the training sample was linked to the OSAVI of
324 December 2004. Confusion with club-rush in 2006 was probably related to the use of an October
325 image instead of September, the confidence interval reaching the splitting value of the MNDWI
326 in October 2006 but not September 2005 (Figs. 6-7). Confusion between reed and agricultural
327 crops (namely sun flower) could be related, at least partially, to the presence of reed at the edge
328 of crops, such as revealed by our field validation in 2006. Reed also grows between rows of vines
329 (8.1% mixed with common reed in 2006) when they are not treated with herbicides and flooded
330 in winter, a common practice in the Camargue.

331 For macrophyte bed discrimination, the values of B4 in December were close to those of
332 sea, club-rush and saline marshes, which are the wettest habitats in our samples. The selection of
333 B4 in December at the first node of the tree was most likely related to the high water levels
334 observed in macrophyte marshes at that period, translating into the lowest mid-infrared values.
335 The NDWIF usually classifies water in positive values and, chlorophyll *a* and turbid
336 environments in negative values (McFeeters, 1996). Hence, the NDWIF discriminates aquatic

337 beds from open-water marshes. This index also combines information about B1 and B3 that are
338 respectively linked to the variable density and the submersion depth of aquatic macrophytes
339 (Lieutaud & Puech, 1996). The values for aquatic beds lie between those of open water (eg., sea)
340 and habitats with a dense vegetation cover. Land covers presenting a mixture of water and sparse
341 vegetation (eg., salt pans and club-rush marshes) were indeed within the same range of values
342 than aquatic macrophytes. Pinnel (2006) observed that the spectra of submerged macrophytes in
343 lakes were influenced by canopy structure, chlorophyll absorption, and secondarily
344 photosynthetic pigments. B2 of SPOT-5 is a chlorophyll-absorption band important for
345 vegetation discrimination. Hence, the new emergence of submerged macrophytes in early fall
346 following water inputs in hunting marshes induces a particular spectral response and explains the
347 selection of both NDWIF and B2 in September for their discrimination. The selection of the SR
348 of March is related to one plot of the training sample that changed markedly between summer
349 2004 and 2005, with a replacement of pondweeds by Eurasian water milfoils after a salinity
350 decrease. This index reveals the contrast between soil and vegetation (Pearson & Miller, 1975),
351 and its value for aquatic bed is unique compared to other land cover classes. Water levels were
352 unusually low in winter 2004-2005, inducing a muddy aspect of the marsh with limited
353 underwater light availability for plants. A gradual increase in water levels during February-March
354 2005 allowed the development of Eurasian water milfoils, well adapted to rapid growth in
355 eutrophic marshes. Hence, it appears that the SR of March permitted the selection of the few
356 turbid, muddy marshes in winter prior to the development of aquatic vegetation.
357 In both the training and validation samples, the predictive variables selected for
358 discrimination of macrophyte beds did not allow their differentiation from saline and club-rush
359 marshes. However, our training sample included predominantly permanent marshes, and
360 misclassifications could be partly explained by the tendency of submerged plants *(Chara,*

Potamotegon, Ruppia) to also develop in temporary marshes assigned to the categories of club-rush, saline marsh and salt pan. For instance, we observed an 80% percent cover of submerged macrophytes in some club-rush beds when they were flooded in spring. Confusion with riparian forest and tamarisk could be explained by digitizing inaccuracies.

Overall accuracy, omission and commission error rates are recommended as primary measures for thematic classification accuracy (Liu et al., 2007). Commission rates, which are useful for understanding the precision of boundaries delineation, are rarely addressed in studies of wetland classification, potentially because they are sensitive to unbalanced classes (Wright & Gallant, 2007). Rutchey & Vilcheck (1999) classified and recoded a SPOT scene that provided a commission error rate of 29% for various densities of cattail, from which an overall error rate of 17% could be calculated. Using the combination of spectral bands and textural features (Landsat TM, SPOT and IRS scenes), Arzandeh & Wang (2003) could map reed stands with a minimum commission error rate of 25%. Broun de Colstoun et al. (2003) obtained a commission error rate of 10% for a wetland class using classification tree and two Landsat (ETM) scenes. Baker et al. (2006) classified wetlands with a commission error rate of 21% and 24%, using CTs alone and with a classification algorithm based on stochastic gradient boosting, respectively. When discriminating wetlands from uplands using CTs and ancillary data, Wright & Gallant (2007) obtained a minimum commission error rate of 40% with an overall error rate of 7%. Using multiseason Quickbird multispectral imagery with an unsupervised classification of eight classes, Ghioca-Robrecht et al. (2008) obtained commission error rates of 24% for common reed and 48% for cattail, from which a 24%overall error rate could be calculated. Our reedbed maps presented an overall accuracy of 99 and 98%, with a commission error of 23 and 30%, and an overall error of 2 and 2% in 2005 and 2006, respectively. These results are amongst the most accurate for mapping wetland emergent vegetation that could be found in the literature, providing a robust

385 tool for reedbed monitoring and management (Story & Congalton 1986). Our estimation of total
386 reed area in the Camargue is close to the 8000 ha estimated by Mathevet & Sandoz (1999), when
387 taking into account the smaller geographic area considered by these authors, which would lead to
388 8204 (2005) and 8334 (2006) ha of reedbeds using our approach. These authors used a supervised
389 classification with the maximum-likelihood algorithm applied to a Landsat TM scene of July
390 1995, eliminated the cropland layer from the scene following the high confusion with ricefields,
391 and corrected the resulting map based on expert knowledge (A. Sandoz, pers. comm.).
392 Unfortunately, the different approaches used prevent us from concluding about changes in reed
393 area over this ten-year period.
394 Our maps of submerged macrophytes presented an overall accuracy of 87 and 86% with a
395 commission error of 64 and 55%, and an overall error of 13 and 14% in 2005 and 2006,
396 respectively. These commission error rates could presumably be improved by integrating the
397 macrophytes developing into temporarily flooded marshes currently classified as club-rush, saline
398 marshes and salt pans. Coverage estimation of submerged macrophytes over an area comprising
399 hundreds of marshes characterized by different abiotic and biotic conditions (water depth,
400 salinity, hydroperiods, aquatic fauna, grazing pressure, etc) had never been done to our
401 knowledge. Such dynamic vegetation that develops asynchronously under water is particularly
402 difficult to monitor, whether from ground survey, aerial photographs or satellite data (Vis et al.,
403 2003; Valley et al., 2005). Estimation of the area covered by submerged macrophytes in the
404 Camargue is a major conservation issue given the socio-economic importance of this habitat for
405 waterfowl hunting and its vulnerability to invasive species such as the emergent plant *Ludwigia*
406 *spp*. or the Louisiana red-swamp crayfish *Procambarus clarkii*. The total area of submerged
407 macrophyte beds in the Camargue was estimated at 29 244 ha in 2005 and 33 797 ha in 2006.
408 The 2006 increase is largely imputable to the confusion with seagrass in the Vaccarès lagoon that

represents 3101 ha in 2006.

CTs have previously provided good accuracies for remote-sensing data especially with multi-date LANDSAT datasets (Brown de Colstoun et al., 2003; Baker et al., 2006). This study is original for having used higher-resolution images combined with thorough field campaigns and a wide variety of multispectral and multiseasonal indices as predictive variables. Likewise, our model performance was not influenced by reed biomass, which affects reflectance (Valta-Hulkkonen et al., 2003) requiring several density classes for good classification accuracy in other studies (Maheu-Giroux & De Bois, 2005).

CTs are considered as especially robust with small samples of remotely-sensed data (Tadjudin & Landgrebe, 1996). To our knowledge, the smallest sample used for testing CT reliability was fifty observations (Brostaux, 2005), and we found no study explaining the impact of an extremely rare class in an unbalanced sample. McIver & Friedl (2002) showed that prior probabilities can be a good solution for not penalizing small classes under a non-parametric classification and observed that adding a prior parameter helped to distinguish hardly separable classes of remote-sensing data, affecting only areas overlapping between two classes. Our results demonstrate that CTs used with an adjusted prior parameter provide reliable models for an unbalanced sample when the smallest class contains as few as 25 observations.

Since our objective was to develop re-applicable and easy interpretable models with good accuracies, we chose to enhance the performance of CTs by cross-validation and priority probabilities that are particularly well suited for data difficult to collect. The CV-1SE pruning method makes the CT approach even more robust, under the assumption that the training sample is representative of the underlying population (Esposito et al., 1999). Cross-validation, jackknifing and bootstrapping have been widely used in estimating prediction errors in many statistical models based on regression and classification (Wintle et al., 2005). However, to ensure

433 that the inferred relationships are robust and the predictions reliable, models should ideally be
434 tested on a completely independent dataset comprising ground validation data collected expressly
435 for such purposes in areas not sampled for the original model derivation (Muller et al., 1998;
436 Congalton & Green, 1999; Wintle et al., 2005; Thomson et al., 2007). Our models were validated
437 with a completely independent set of images and field data, complemented with a comparative
438 analysis of the mean reflectance (and confidence interval) of each land cover type. Model
439 usefulness also depends on the "time-robustness" and "space-robustness" of the model itself and
440 of its predictive variables. In Camargue marshes, the vegetation development is related to
441 seasonal rainfall and human interventions, which are highly variable in time and space
442 (Chauvelon, 2009). The training and validation years differed in their rainfall regime (664 mm in
443 2005 vs 411 mm in 2006, with 72% of this difference being attributed to April-May) certainly
444 affecting the seasonal development of marsh vegetation. In spite of these annual differences, our
445 training sample based on a single year provided robust models, with CTs integrating different
446 types of wetland hydrology and phenology.

447 According to DongMei & Douglas (2002), different sampling protocols might have more
448 impact on the resulting classification when a finer resolution is used. Additional field campaigns
449 addressing other land use types would certainly contribute to improve the accuracy of our
450 models. Likewise, the lack of a September image for the 2006 validation sample decreases the
451 accuracy of our models, highlighting the importance of using pre-programmed scenes of which
452 the date is carefully selected based on phelonogical/hydrological events.

453 Satellite remote sensing techniques have often been criticized in the past because they
454 lacked the necessary resolution for wetland spatial analysis (see Özesmi & Bauer, 2002). The
455 resolution of SPOT-5 scenes provides an adequate scale for acquiring detailed field data within
456 homogeneous stands, allowing to optimize the time spent for data collecting and to properly

457 locate the sampled plots on the ground and on the scenes. Remote sensing has often been seen as
458 a complementary tool to conventional mapping techniques (Girard & Girard, 1999; Özesmi &
459 Bauer, 2002). Our results demonstrate that it is possible with a good field campaign to avoid
460 repeated sampling for long-term cost-efficient monitoring, with four scenes being sufficient for a
461 follow-up of emergent and submerged macrophytes in the Camargue. A programmed SPOT-5
462 scene costs 250 € (with ISIS funding) or 2700 € (full price), which is less than the costs
463 associated with a complete photographic aerial coverage, not to mention the time further required
464 for image interpretation, digitalization and field validation. The accuracy and reliability of our
465 models provide a vision where the roles are reversed: the field campaigns become a
466 complementary tool in wetland monitoring using satellite remote sensing.
467
468 **Acknowledgements**
469
470 We are indebted to the Centre National d'Études Spatiales (CNES) for funding the
471 programming and acquisition of SPOT scenes (ISIS Projects 698 & 795), to the Office National
472 de la Chasse et de la Faune Sauvage (ONCFS) for providing a thesis grant to A. Davranche, to
473 the Foundation Tour duValat for logistic support and to the Parc Naturel Régional de Camargue
474 (PNRC) and the Syndicat Mixte of the Camargue Gardoise (SMCG) for providing the vector
475 layers of land cover types in 2001 and 2006 (Conventions N°*241-2007-04)*. Thanks are extended
476 to A. Sandoz and M. Pichaud for their technical support and to E.Duborper, J-B Mouronval, J-Y
477 Mondain-Monval, C. Nourry, A. Diot, J. Desgagné, M. Gobert, S. Didier, L.Malkas, for their
478 contribution to field . We are also grateful to the managers of Tour du Valat, Marais du Vigueirat,
479 Palissade, Camargue Gardoise (Maire de Vauvert and SMCG) and to private landowners for
480 granting us access to their marshes and providing hydrological data. A special thanks to L.

Landenburger for her advice on using classification trees.

References

Arzandeh, S., & Wand, J. (2003) Monitoring the change of *Phragmites* distribution using satellite data. *Canadian Journal of Remote Sensing*, 29, 24-35.

Baker, C., Lawrence, R., Montagne, C., & Patten, D. (2006). Mapping wetlands and riparian areas using Landsat ETM+ imagery and Decision-Tree-Based models. *Wetlands*, 26, 465-474.

Baret, F., & Weiss, M. (2004). *Can-Eye: processing digital photographs for canopy structure characterization, Tutorial* (http://www.avignon.inra.fr/can_eye/page2.htm).

Bradley, B. A., & Fleishman, E. (2008). Can remote sensing of land cover improve species distribution modelling? *Journal of Biogeography*, 35, 1158-1159.

Breiman, L., Friedman, J. H., Olshen, R., & Stone, C. (1984). *Classification and regression trees*. Chapman & Hall, New York, USA.

Brostaux, Y. (2005). *Etude du classement par forêt aléatoire d'échantillons perturbés à forte structure d'intéraction*. PhD thesis, Faculté des sciences agronomiques de Gembloux, Communauté Française de Belgique.

Brown de Colstoun, E. C., Story, M. H., Thompson, C., Commisso, K., Smith, T. G., & Irons, J. R. (2003). National Park vegetation mapping using multi-temporal Landsat 7 data and a decision tree classifier. *Remote Sensing of Environment*, 85, 316-327.

Caillaud, L., Guillaumont, B., & Manaud, F. (1991). *Essai de discrimination des modes d'utilisation des marais maritimes par analyse multitemporelle d'images SPOT. Application aux marais maritimes du Centre Ouest*. IFREMER, (H4.21) 485. 24 p.

505 Chauvelon, P., 2009. Gestion Intégrée d'une Zone humide littorale méditerranéenne aménagée :
506 contraintes, limites et perspectives pour l'Ile de CAMargue (GIZCAM). Programme LITEAU
507 2, Ministère de l'Ecologie, de l'Energie, du Développement durable et de l'Aménagement du
508 Territoire, Final report, Tour du Valat, 84 pp.
509 Congalton, R. G., & Green, K. (1999). *Assessing the accuracy of remotely sensed data:*
510 *Principles and practices*. Boca Raton, FL: CRC Press.
511 Davranche, A., Lefebvre, G., & Poulin, B. (2009). Radiometric normalization of multi-temporal
512 SPOT 5 images for wetland monitoring : accuracy of pseudo-invariant features vs. 6S
513 atmospheric model. *Photogrammetric engineering and remote sensing*, 75, 723-729.
514 DongMei, C., & Douglas, S. (2002). The effect of training strategies on supervised classification
515 at different spatial resolutions. *Photogrammetric Enginering and Remote Sensing*, 68, 1155-
516 1161.
517 Esposito, F., Malerba, D., Semeraro, G., & Tamma, V. (1999). The effects of pruning methods on
518 the predictive accuracy of induced decision trees. *Applied Stochastic Models in Business and*
519 *Industry*, 15, 277-299.
520 Gao, B. G. (1996). NDWI-a normalized difference water index for remote sensing of vegetation
521 liquid water from space. *Remote Sensing of Environment*, 58, 257-266.
522 Ghioca-Robrecht, D. M., Johnston, C. A., & Tulbure, M. G. (2008). Assessing the use of
523 multiseason Quickbird imagery for mapping invasive species in a lake Erie coastal marsh.
524 *Wetlands*, 28, 1028-1039.
525 Girard, M. C., & Girard, C. M. (1999). *Traitement des données en télédétection*. Éditions Dunod,
526 Paris.
527 Gond, V., Bartholome, E., Ouattara, F., Nonguierma, A., & Bado, L. (2004). Surveillance et
528 cartographie des plans d'eau et des zones humides et inondables en régions arides avec

529 l'instrument VEGETATION embarqué sur SPOT-4. *International Journal of Remote*
530 *Sensing*, 25, 987–1004.
531 Grillas, P. (1992). *Les communautés de macrophytes submergées des marais temporaires oligo-*
532 *halins de Camargue. Etude expérimentale des causes de la distribution des espèces*. PhD
533 Thesis, University of Rennes 1.
534 Hanqiu, X. (2006). Modification of Normalized Difference Water Index (NDWI) to enhance
535 open water features in remotely sensed imagery. *International Journal of Remote Sensing*, 27,
536 3025 – 3033.
537 Harrell, F. E. J. (2001). *Regression Modeling Strategies. With Applications to Linear Models,*
538 *Logistic Regression, and Survival Analysis*. Springer Series in Statistics, Springer, New York
539 Huete, A. R. (1988). A Soil-Adjusted Vegetation Index (SAVI). *Remote sensing of Environment*,
540 25, 295-309.
541 Hunt, E. R., & Rock, B. N. (1989). Detection of Changes in Leaf Water Content Using Near- and
542 Middle-infrared Reflectances. *Remote Sensing of Environment*, 30, 43-54.
543 Johnston, R. M., & Barson, M. M. (1993). Remote sensing of Australian wetlands: An evaluation
544 of Landsat TM data for inventory and classification. *Australian Journal of Marine and*
545 *Freshwater Research*, 4, 235–252.
546 Lawrence, R., Bunn, A., Powell, S., & Zambon, M. (2004). Classification of remotely sensed
547 imagery using stochastic gradient boosting as a refinement of classification tree analysis.
548 *Remote Sensing of Environment*, 90, 331–336.
549 Lillesand, T. M., & Kiefer, R. W. (1987). *Remote sensing and image interpretation, 2nd edition.*
550 John Wiley and Sons, New York.
551 Lieutaud, A., & Puech, C. (1996). Méthode de traitement d'images adaptée au capteur SPOT
552 pour une cartographie quantitative des herbiers lagunaires submergés. *Bulletin de la Société*

française de photogrammétrie et de télédétection, 141, 115-120.

Maheu-Giroux, M., & De Bois, S. (2005). Mapping the invasive species *Phragmites australis* in linear wetland corridors. *Aquatic Botany*, 83, 310-320.

Mathevet, R., & Sandoz, A. (1999). L'exploitation du roseau et les mesures agri-environnementales dans le delta du Rhône. *Revue de l'Economie Méridionale*, 47 (185-186), 101-122.

McFeeters, S. K. (1996). The use of the normalised difference water index (NDWI) in the delineation of open water features. *International Journal of Remote Sensing*, 17, 1425–1432.

McIver, D. K., & Friedl, M. A. (2002). Using prior probabilities in decision-tree classification of remotely sensed data. *Remote Sensing of Environment*, 81, 253– 261.

Özesmi, S. L. (2000). Satellite Remote Sensing of Wetlands and a Comparison of Classification Techniques, PhD Thesis, University of Minnesota.

Özesmi, S. L., & Bauer, M. E. (2002). Satellite remote sensing of wetlands. *Wetlands Ecology and Management*, 10, 381–402.

Pearson, R. L., & Miller, L. D. (1972). *Remote mapping of standing crop biomass for estimation of the productivity of the short-grass Prairie, Pawnee National Grasslands, Colorado.* Processing of the 8th International Symposium on Remote Sensing of Environment, ERIM, Ann Arbor, MI, 1357-1381.

Pinnel, N. (2007). *A method for mapping submerged macrophytes in lakes using hyperspectral remote sensing*. Phd Thesis, Technische Universität München.

Ramsey, E. W., & Laine, S. C. (1997). Comparison of Landsat Thematic Mapper and high resolution aerial photography to identify change in complex coastal wetlands. *Journal of Coastal Research*, 13, 281–92.

Richardson, A. J., & Everitt, J. H. (1992). Using spectra vegetation indices to estimate rangeland

productivity. *Geocarto International*, 1, 63-69.

Rondeaux, G., Steven, M., & Baret, F. (1996). Optimization of Soil-Adjusted Vegetation Indices. *Remote Sensing of Environment*, 55, 95-107.

Rouse, J. W., Haas, R. H., Schell, J. A., & Deering, D. W. (1973). Monitoring vegetation systems in the great plains with ERTS, Third ERTS Symposium, *NASA SP-351*, 1, 309-317.

Sader, S. A., Ahl, D., & Wen-Shu, L. (1995). Accuracy of Landsat-TM and GIS Rule-Based Methods for Forest Wetland Classification in Maine. *Remote Sensing of the Environment*, 53, 133-144.

Schmidt, K. S., & Skidmore, A. K. (2003). Spectral discrimination of vegetation types in a costal wetland. *Remote Sensing of Environment*, 85, 92-108.

Silvestri, S., Marani, M., Settle J., Benvenuto, F., & Marani, A. (2002). Salt marsh vegetation radiometry: data analysis and scaling, *Remote Sensing of Environment*, 2, 473-482.

Sivanpillai, R., & Latchininsky, A. V. (2007). Mapping locust habitat in the Amudarya river delta, Uzbekistan with multi-temporal MODIS imagery. *Environmental Management*, 39, 876-886.

Sokal, R. R., & Rohlf, F. J. (1995). *Biometry: The principles and practices of statistics in biological research.* NY: W.H. Freeman.

Spot Image (2008). *Preprocessing levels and location accuracy.* Technical information, www.spotimage.com

Story, M., & Congalton, R. G. (1986). Accuracy assessment: A user's perspective. *Photogrammetric Engineering and Remote Sensing*, 52, 397−399.

Tadjudin, S., & Landgrebe, D. A. (1996). A decision tree classifier design for high-dimensional data withlimited training samples. Geoscience and Remote Sensing Symposium, 1996. IGARSS 96. *Remote Sensing for a Sustainable Future International*, 1(27-31), 790 – 792.

601 Tamisier, A., & Grillas, P. (1994). A review of habitat changes in the Camargue : an assessment
602 of the effects of the loss of biological diversity on the wintering waterfowl community.
603 *Biological Conservation*, 70, 39-47.
604 Therneau, T. M., & Atkinson, E. J. (1997). *An Introduction to Recursive Partitioning Using the*
605 *RPART Routines.* Mayo Foundation (http://www.mayo.edu/hsr/techrpt/61.pdf).
606 Thomson, J., Mac Nally, R., Fleishman, E., & Horrocks, G. (2007). Predicting bird species
607 distributions in reconstructed landscapes. *Conservation Biology*, 21, 752–66.
608 Valley, R. D., Drake, M. T., & Anderson, C. S. (2005). Evaluation of alternative interpolation
609 techniques for the mappig of remotely-sensed submersed vegetation abundante. *Aquatic*
610 *Botany*, 81, 13-25.
611 Valta-Hulkkonen, K., Pellikka, P., Tanskanen, H., Ustinov, A., & Sandman, O. (2003). Digital
612 false colour aerial photographs for discrimination of aquatic macrophyte species. *Aquatic*
613 *Botany*, 75, 71-88.
614 Vermote, E. , Tanre, D., Deuze, J. L., Herman, M., & Morcrette, J. J. (1997).Second simulation
615 of the satellite signal in the Solar Spectrum, 6S: An overview. *IEEE Transactions on*
616 *Geoscience and Remote Sensing*, 35, 675-686.
617 Vis, C., Hudon, C., & Carignan, R. (2003). An evaluation of approaches used to determine the
618 distribution and biomass of emergent and submerged aquatic macrophytes over large spatial
619 scales. *Aquatic Botany*, 77, 187-201.
620 Wintle, B. A., Elith, J., & Potes, J. (2005). Fauna habitat modelling and mapping; A review and
621 case study in the Lower Hunter Central Coast of NSW. *Austral Ecology*, 30, 719-738
622 Wright, C., & Gallant, A. (2007). Improved wetland remote sensing in Yellowstone National
623 Park using classification trees to combine TM imagery and ancillary environmental data.
624 *Remote Sensing of Environment*, 107, 582-605.

Table 1

Multispectral indices used in this study.

Indices	Formula	References
SR - Simple Ratio	B2/B3	Pearson & Miller, 1972
VI - vegetation index	B3/B2	Lillesand & Kiefer, 1987
DVI - Differential Vegetation Index	B3-B2	Richardson & Everitt, 1992
MSI - Moisture Stress Index	B4/B3	Hunt & Rock, 1989
NDVI - Normalized Difference Vegetation Index	(B3-B2)/(B3+B2)	Rouse et al., 1973
SAVI - Soil Adjusted Vegetation Index	1.5*(B3-B2)/(B3+B2+0.5)	Huete, 1988
OSAVI – Optimized SAVI	(B3-B2)/(B3+B2+0.16)	Rondeaux *et. al*., 1996
NDWI – Normalized Difference Water Index	(B3-B4)/(B3+B4)	Gao, 1996
NDWIF – Normalized Difference Water Index of Mc Feeters	(B1-B3)/(B1+B3)	Mc Feeters, 1996
MNDWI – Modified Normalized Difference Water Index	(B1-B4)/(B1+B4)	Hanqiu, 2006
DVW – Difference between Vegetation and Water	NDVI - NDWI	Gond *et al*, 2004

Table 2

Error rates and accuracy for maps of reed and aquatic beds in 2005 and 2006.

	Omission error (%)		Overall accuracy (%)	Commission error (%)		Overall error (%)
	Reedbeds	Other land covers		Reedbeds	Other land covers	
2005	16.7	1.4	98.6	22.9	1.0	2.2
2006	11.5	1.9	98.1	29.7	0.6	2.4
	Aquatic beds	Other land covers		Aquatic beds	Other land covers	
2005	10.1	13.3	86.7	64.2	1.0	13.1
2006	16.2	14.1	85.9	55.4	2.5	14.4

Table 3

Omission error rates (%) for reed and aquatic beds in 2005 and 2006 relative to other land cover types.

Land cover types		2005		2006	
		Map of common reed (Total class: 1.4 %)	Map of submerged macrophytes (Total class: 13.3 %)	Map of common reed (Total class: 1.9 %)	Map of submerged macrophytes (Total class: 14.1 %)
Sea	6362	0.0	0.0	0.0	0.1
Submerged macrophytes	99	0.0		0.0	
Common reed	30		0.0		0.0
Tamarisk	1264	18.8	1.0	16.1	9.1
Riparian forest	8822	8.8	0.4	1.4	6.9
Sawgrass	93	0.0	0.0	0.0	0.0
Rush	6236	0.5	0.8	2.1	2.1
Grassland	8631	0.7	0.1	0.6	0.3
Sand	5370	0.1	2.5	0.5	1.1
Saline marsh	98047	0.0	26.4	0.0	24.1
Salt pan	42248	1.5	5.3	0.9	13.0
Urban	6669	4.5	0.0	4.7	0.0

Table 3. continued

Club rush	9	0.0	44.4	30.0	77.8
Other forests	3017	1.0	0.0	0.7	2.9
Sunflower	1709			23.2	0.0
Wheat	1241			5.4	0.0
Orchard	2319			0.0	0.0
Rape	1359			0.0	0.0
Vines	1395			8.4	0.0
Market gardening	611			3.8	0.0
Fallow land	2468			0.2	0.0
Corn	2031			0.2	0.0
Ploughed crop	746			13.5	0.0
Meadow	498			0.0	0.0
Rice	13278			7.8	0.0
All crops	27655	3.1	1.4	6.3	0.0

Table 4

Contribution of plant structure and hydrology to habitat misclassification (Likelihood-ratio test).

Structural parameters	Difference of scaled deviances	df	*P*
Common reed			
Height of green stems	0.0885	1	*0.766*
Density of green stems	0.0705	1	*0.791*
Density of dry stems	0.3918	1	*0.531*
Ratio dry/green stems	0.8777	1	*0.349*
Diameter of green stems	0.2088	1	*0.648*
Diameter of dry stems	0.0026	1	*0.960*
Homogeneity	0.0230	1	*0.879*
Vegetation cover rate	0.7578	1	*0.384*
Year	6.2118	1	*0.013*
Submerged macrophytes			
Percent cover of submerged species	15.083	1	*0.0001*
Water level	0.446	1	*0.504*
Salinity	11.015	1	*0.001*
Water turbidity	11.186	1	*0.001*
Proportion of plants showing on the water surface	17.174	1	*3.411*
Submerged species	0.83	1	*0.362*
Year	6.175	1	*0.013*

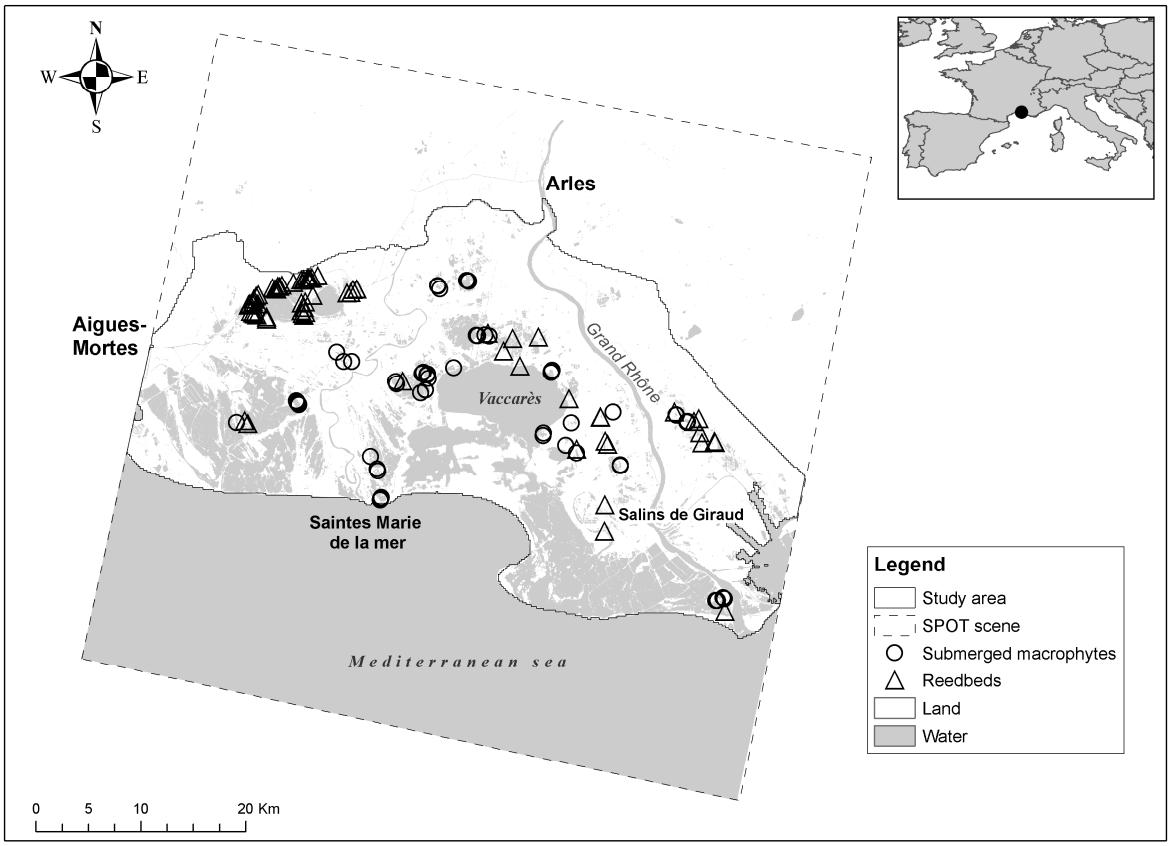

Fig. 1. Distribution of the 175 study plots (training and validation samples) of reeds and submerged macrophytes in the Camargue.

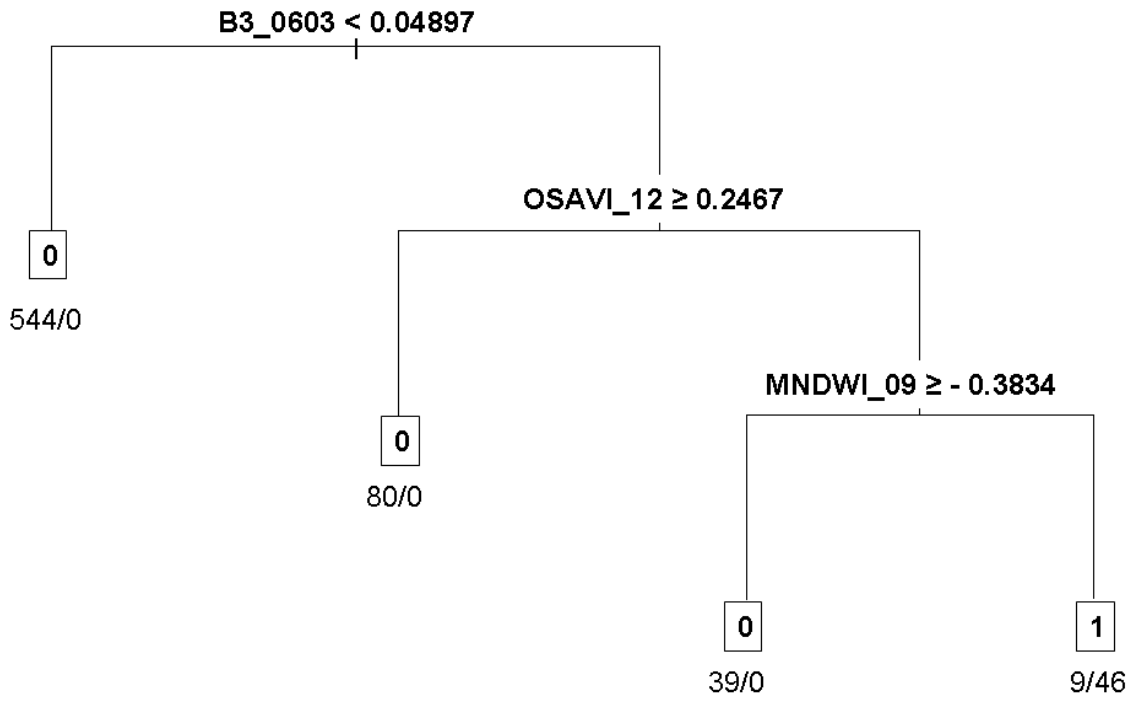

Fig. 2. Optimal tree for common reed classification. Presence of common reed = 1, presence of other land covers = 0. The number of sites assigned to 0 (on the left) and 1 (on the right) is indicated below each end node.

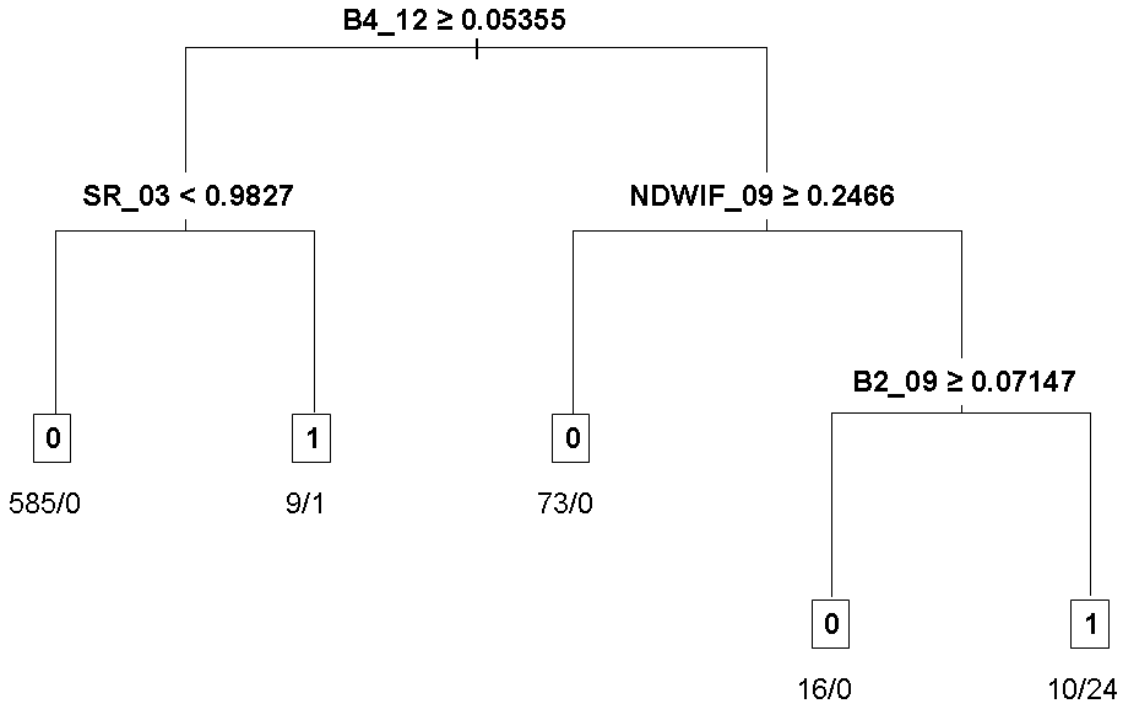

Fig. 3. Optimal tree for the classification of submerged macrophytes. Presence of submerged macrophytes = 1, presence of other land covers = 0. The number of sites assigned to 1 and 0 (1/0) is indicated for each terminal node.

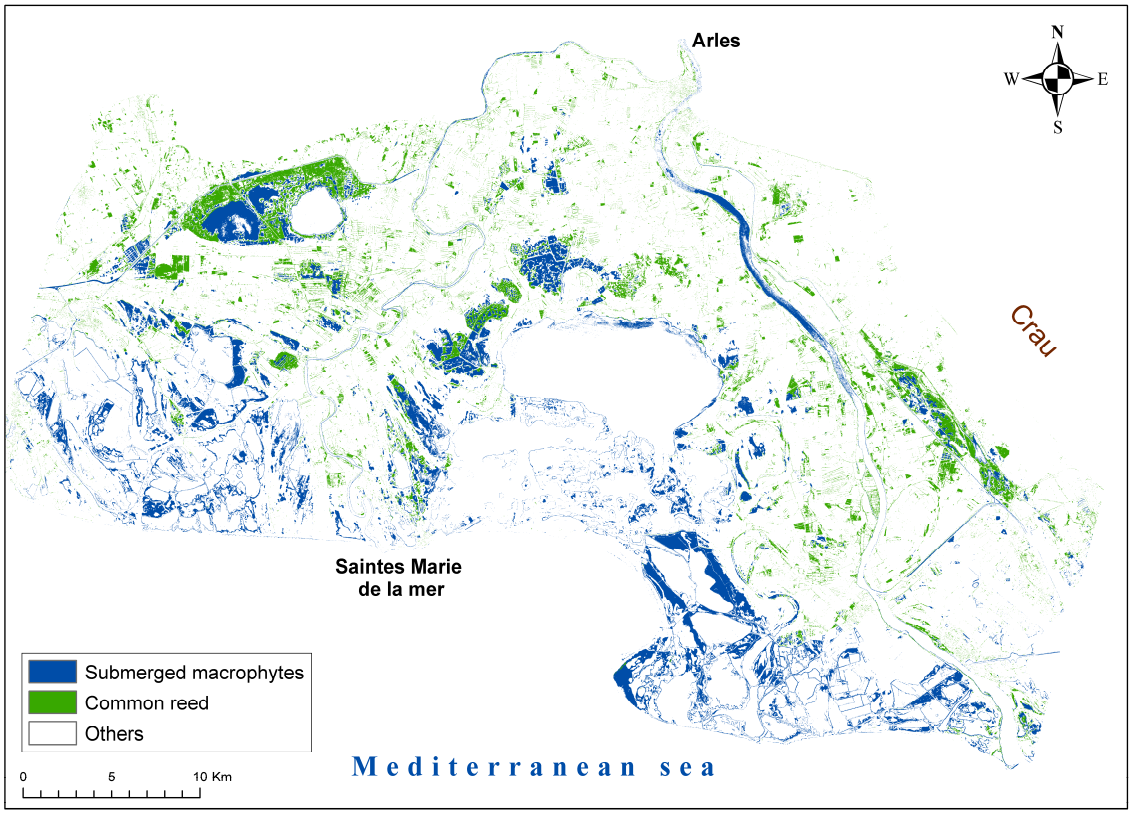

Fig. 4. Distribution map of common reed and submerged macrophytes in the Camargue in 2005.

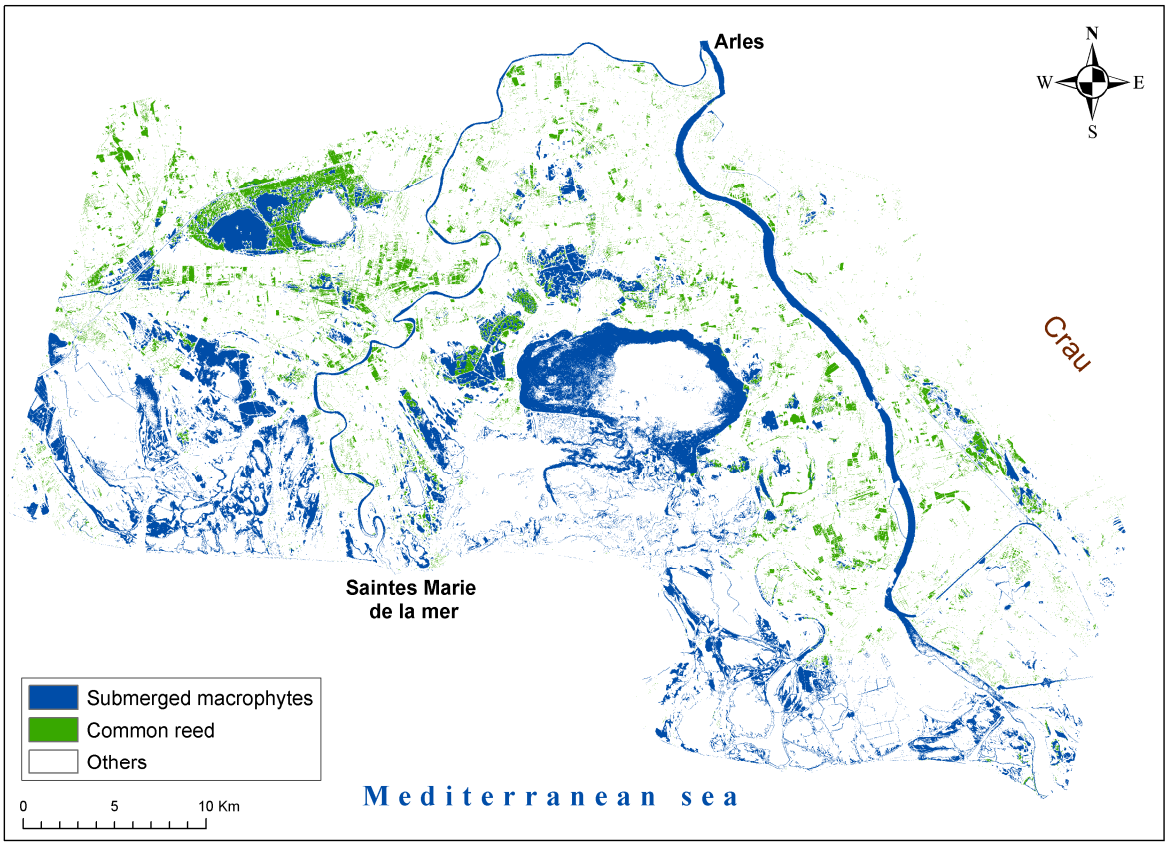

Fig. 5. Distribution map of common reed and submerged macrophytes in the Camargue in 2006.

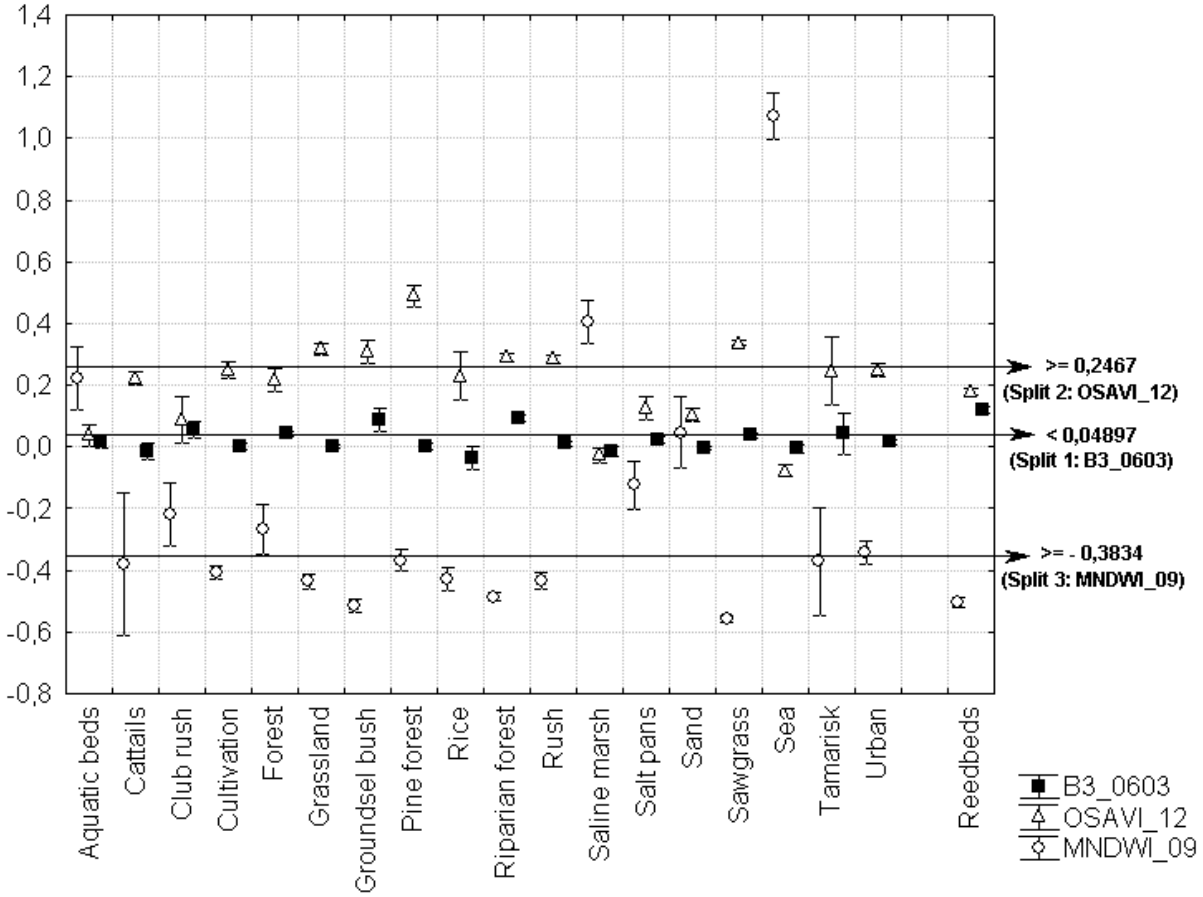

Fig. 6. Mean values and confidence intervals (95%) of each predictive variable in the reedbed model for each land cover class of the training sample (2005).

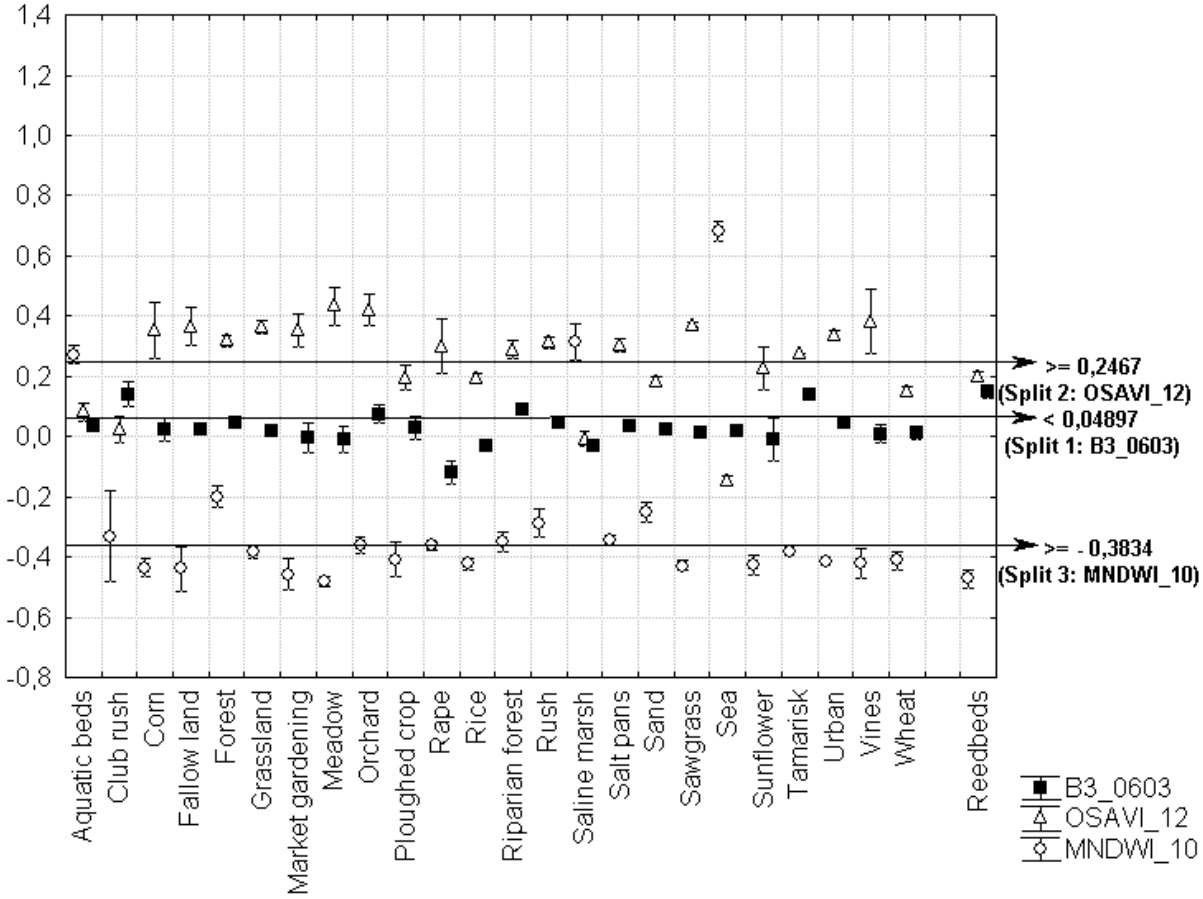

Fig. 7. Mean values and confidence intervals (95%) of each predictitive variable in the reedbed model for each land cover class in the validation sample (2006)

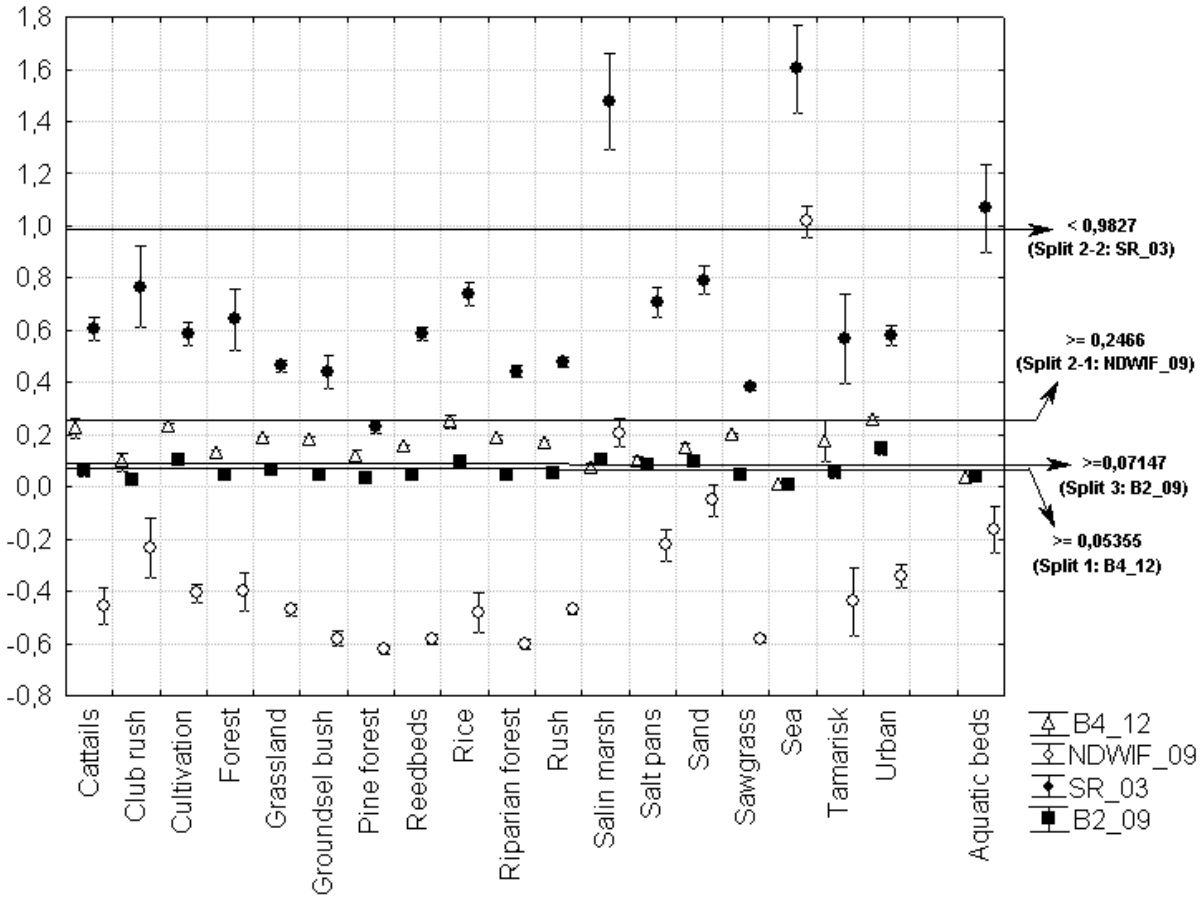

Fig. 8. Mean values and confidence intervals (95%) of each predictive variable in the aquatic bed model for each land cover class in the training sample (2005).

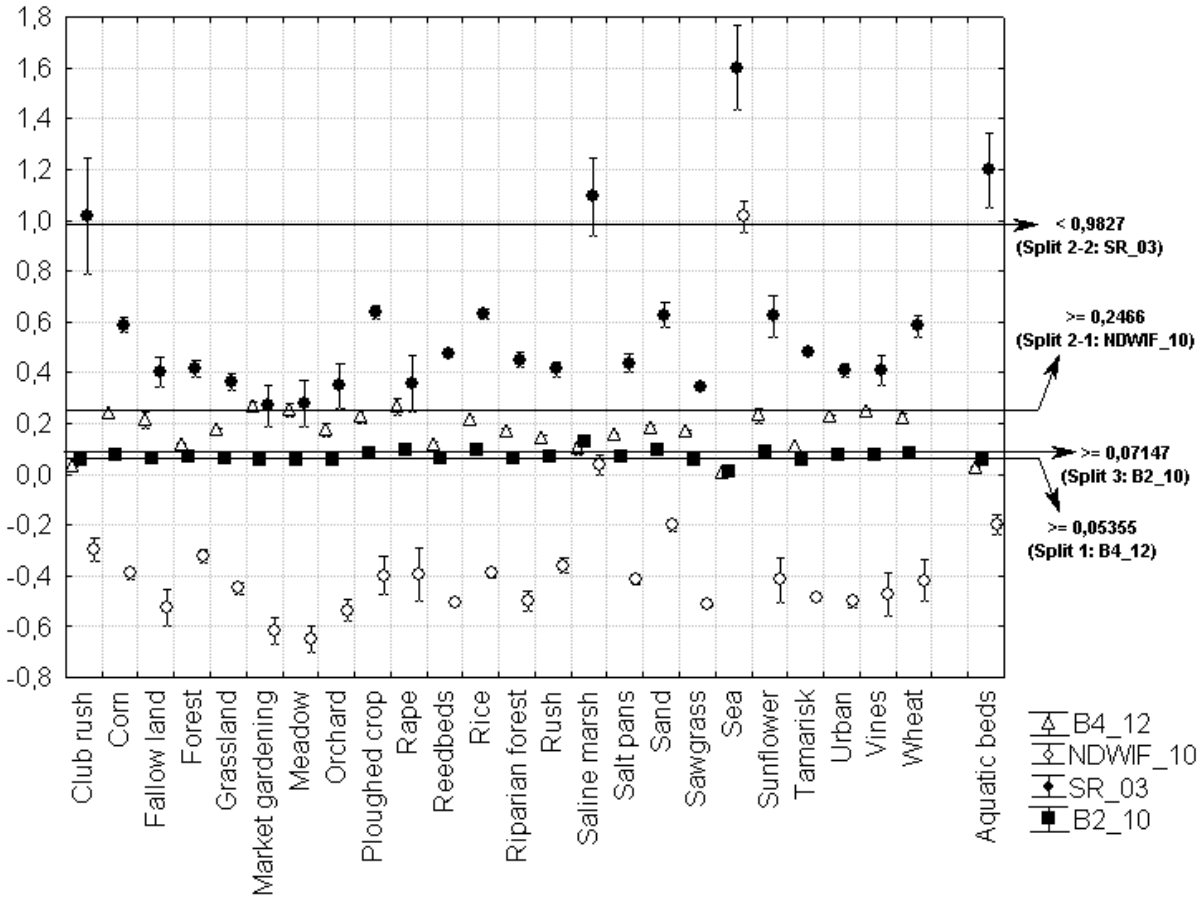

Fig. 9. Mean values and confidence intervals (95%) of each predictive variable in the aquatic-bed model for each land cover class in the validation sample (2006).